



HAL
open science

Multiple evolutionary origins and losses of tooth complexity in squamates

Fabien Lafuma, Ian J Corfe, Julien Clavel, Nicolas Di-Poï

► **To cite this version:**

Fabien Lafuma, Ian J Corfe, Julien Clavel, Nicolas Di-Poï. Multiple evolutionary origins and losses of tooth complexity in squamates. *Nature Communications*, 2021, 12 (6001), 10.1038/s41467-021-26285-w . hal-03395195

HAL Id: hal-03395195

<https://hal.science/hal-03395195>

Submitted on 29 Nov 2021

HAL is a multi-disciplinary open access archive for the deposit and dissemination of scientific research documents, whether they are published or not. The documents may come from teaching and research institutions in France or abroad, or from public or private research centers.

L'archive ouverte pluridisciplinaire **HAL**, est destinée au dépôt et à la diffusion de documents scientifiques de niveau recherche, publiés ou non, émanant des établissements d'enseignement et de recherche français ou étrangers, des laboratoires publics ou privés.

Multiple evolutionary origins and losses of tooth complexity in squamates

Fabien Lafuma ^{1✉}, Ian J. Corfe ^{1,2✉}, Julien Clavel^{3,4} & Nicolas Di-Poi ^{1✉}

Teeth act as tools for acquiring and processing food, thus holding a prominent role in vertebrate evolution. In mammals, dental-dietary adaptations rely on tooth complexity variations controlled by cusp number and pattern. Complexity increase through cusp addition has dominated the diversification of mammals. However, studies of Mammalia alone cannot reveal patterns of tooth complexity conserved throughout vertebrate evolution. Here, we use morphometric and phylogenetic comparative methods across fossil and extant squamates to show they also repeatedly evolved increasingly complex teeth, but with more flexibility than mammals. Since the Late Jurassic, multiple-cusped teeth evolved over 20 times independently from a single-cusped common ancestor. Squamates frequently lost cusps and evolved varied multiple-cusped morphologies at heterogeneous rates. Tooth complexity evolved in correlation with changes in plant consumption, resulting in several major increases in speciation. Complex teeth played a critical role in vertebrate evolution outside Mammalia, with squamates exemplifying a more labile system of dental-dietary evolution.

¹Institute of Biotechnology, Helsinki Institute of Life Science, University of Helsinki, FI-00014 Helsinki, Finland. ²Geological Survey of Finland, FI-02150 Espoo, Finland. ³Department of Life Sciences, The Natural History Museum, London SW7 5BD, UK. ⁴Univ. Lyon, Université Claude Bernard Lyon 1, CNRS, ENTPE, UMR 5023 LEHNA, F-69622 Villeurbanne, France. ✉email: fabien.lafuma@gmail.com; ian.corfe@gtk.fi; nicolas.di-poi@helsinki.fi

As organs directly interacting with the environment, teeth are central to the acquisition and processing of food, determine the achievable dietary range of vertebrates¹, and their shapes are subject to intense natural selective pressures^{2,3}. Simple conical to bladed teeth generally identify faunivorous vertebrates, while higher dental complexity—typically a result of more numerous cusps—enables the reduction of fibrous plant tissue and is crucial to the feeding apparatus in many herbivores^{2,4,5}. Evidence of such dental-dietary adaptations dates back to the first herbivorous tetrapods in the Palaeozoic, about 300 million years ago (Ma)⁴. Plant consumers with highly complex teeth have subsequently emerged repeatedly within early synapsids⁴, crocodyliforms⁶, dinosaurs^{7–9}, and stem and crown mammals^{10–13}. Since the earliest tetrapods had simple, single-cusped teeth², such examples highlight repeated, independent increases of phenotypic complexity throughout evolution¹⁴. Many such linked increases in tooth complexity and plant consumption have been hypothesised to be key to adaptive radiations^{11,13}, though such links have rarely been formally tested. It is also unclear whether the known differences in tooth development between tetrapod clades might result in differences in the evolutionary patterns of convergent functional adaptations^{15,16}.

To understand the repeated origin of dental-dietary adaptations and their role in vertebrate evolution, we investigated tooth complexity evolution in squamates (“lizards” and snakes), the largest tetrapod radiation. Squamates can have simple teeth in homodont dentitions or complex, multicuspid teeth in heterodont dentitions¹⁷, and squamate ecology spans a broad range of past and present niches. Squamates express dental marker genes broadly conserved across vertebrates¹⁵, with varying patterns of localisation and expression compared to mammals, and structures at least partially homologous to mammalian enamel knots (non-proliferative signalling centres of ectodermal cells) determine tooth shape in some squamate clades^{16,18,19}. In mammals—the most commonly studied dental system—novel morphologies arise from developmental changes in tooth morphogenesis²⁰. Epithelial signalling centres—the enamel knots—control tooth crown morphogenesis²¹, including cusp number and position and ultimately tooth complexity, by expressing genes of widely conserved signalling pathways^{15,22}. Experimental data show most changes in these pathways result in tooth complexity reduction, or complete loss of teeth²². Yet, increasing tooth complexity largely dominates the evolutionary history of mammals^{2,10–13}, and it remains unknown whether similar patterns of tooth complexity underlie all tetrapod evolution or are the specific results of mammalian dental development and history.

Here, we assemble and analyse a dataset of cusp number and diet data for 545 squamate species spanning all the living and extinct diversity of the group since its estimated origin in the Permian²³, including tooth morphometric data for 75 species representing all past and present clades we find to have evolved complex teeth. First, we examine the extent of squamate dental diversity and its distribution throughout the group and test how cusp number and tooth shape relate to squamate diets. We then use phylogenetic comparative methods to investigate the patterns of evolution of tooth complexity and plant consumption and address their connection through evolutionary history. Lastly, we fit two different model frameworks to determine whether dental complexity and diet evolution drove squamate diversification. Our findings show that squamate tooth complexity evolved and was lost numerous times in correlation with the evolution of plant-based diets, with the Late Cretaceous representing a critical time for both traits. The Late Cretaceous was also a crucial period for squamate diversification dynamics, and we find that higher tooth complexity and plant consumption led to higher speciation rates.

Results

Dental-dietary adaptations to plant consumption. Among the 545 fossil and extant squamate species examined, we identified species with multicuspid teeth in 29 of 100 recognised squamate families (Fig. 1a, Supplementary Figs. 1–4, Supplementary Data 1–3). Within extant “lizards”, we found multicuspid species in almost 56% of families (24/43), with three-cusped teeth being most common (67% of multicuspid species). While lacking entirely in mostly predatory clades (dibamids, geckos, snakes), multicuspidness dominates Iguania and Lacertoidea, the two most prominent groups of plant-eating squamates, totalling 72% of all extant omnivores and herbivores (Fig. 1a and Supplementary Data 3). A Kruskal–Wallis test and post hoc pairwise Wilcoxon–Mann–Whitney tests show squamate dietary guilds differ statistically in tooth complexity, with the proportion of multicuspid species and cusp number successively increasing along a plant consumption gradient, from carnivores to insectivores, omnivores, and herbivores (p -value < 0.001 ; Fig. 1b and Supplementary Table 1). We quantified tooth outline shape in a subset of taxa spanning all major multicuspid groups with two-dimensional semi-landmarks (Supplementary Data 4). Along principal component 1 (PC1) of the multicuspid tooth morphospace, tooth protrusion is responsible for the greatest extent of shape variation (80.82%), from low-protruding teeth at negative scores, to high-protruding teeth at positive scores (Fig. 1c). Principal component 2 (PC2, 8.08% of total variance) reflects changes in top cusp angle (i.e., apical flaring), which increases when going from negative to positive scores (i.e., conical to fleur-de-lis-like teeth, Fig. 1c). In contrast to the relatively similar teeth of insectivores and omnivores, the teeth of herbivores occupy a distinct morphospace region of more protruding morphologies with a wider top cusp angle (Fig. 1c). A regularised phylogenetic multivariate analysis of variance (MANOVA) on principal component scores confirms statistically significant differences between diets overall (p -value = $8.0e-04$; Fig. 1c) with negligible phylogenetic signal in the model’s residuals (Pagel’s $\lambda = 0.03$). Herbivore teeth significantly differ from both the insectivorous and omnivorous morphospace regions (Fig. 1c and Supplementary Table 2), similarly to observations from mammals and saurians^{5,17}. Conversely, insectivores and omnivores share a largely overlapping morphospace, which is maintained even in discriminant analysis (DFA; Supplementary Fig. 5).

Patterns in tooth complexity and diet evolution. Using Maximum Likelihood reconstructions of ancestral character states across our squamate phylogeny (Fig. 2, Supplementary Figs. 6 and 7, Supplementary Tables 3 and 4), we found dental-dietary adaptations to plant consumption repeatedly evolved, arising from the convergent evolution of multicuspidness. Since the Late Jurassic, six major clades and 18 isolated lineages independently evolved multicuspid teeth from a unicuspid ancestral morphology, mostly through single-cusp addition events, for a total of 24 independent originations of complex teeth (see Fig. 2 and Supplementary Fig. 6 for the names and positions of major clades 1–6). Similar numbers—10 major clades, 13 isolated lineages—show independent origins of plant consumption from carnivorous or insectivorous ancestors (see Fig. 2 and Supplementary Fig. 6 for the names and positions of major clades 1’–10’). Across the tree, most lineages and terminal taxa are unicuspid insectivores retaining the reconstructed ancestral squamate condition. However, of 102 lineages showing cusp number or plant consumption increases, 42 (41%) of increases are along the same phylogenetic path as an increase in the other character (see Methods; Supplementary Table 5).

Although both tooth complexity and plant consumption first originated relatively early (in the Late Jurassic and Early

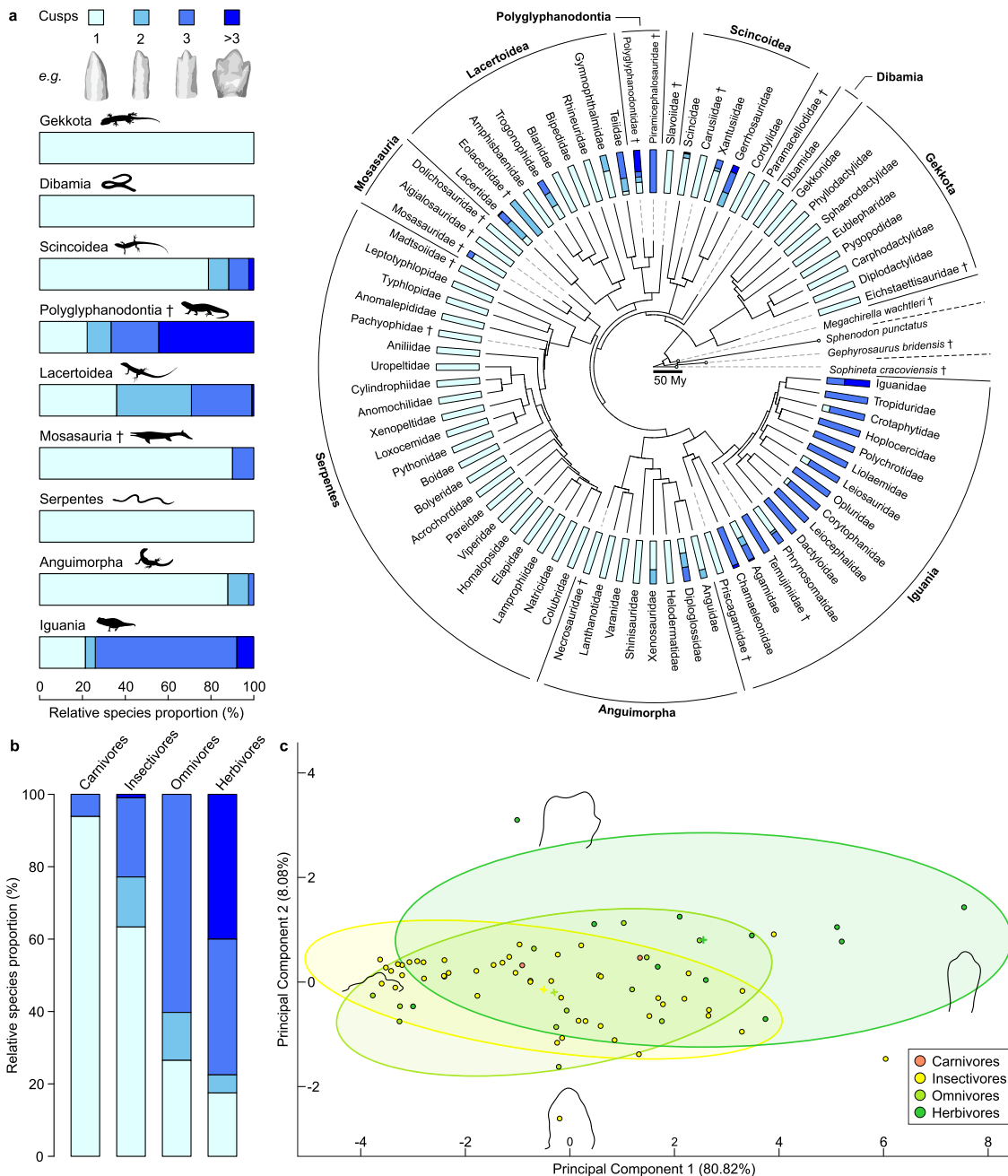


Fig. 1 The diversity of squamate dental morphologies correlates with a gradient of plant consumption. **a** Relative proportions (%) of tooth complexity levels in all known squamate suborders/super-families (left) and 76 families (right) based on cusp number data for 545 living and extinct species (including the most ancient known squamate *Megachirella wachtleri*), two rhynchocephalians, and the stem lepidosaurian *Sophineta cracoviensis*, with example teeth for each complexity level redrawn from microCT-scan data (not to scale). **b** Relative proportions (%) of tooth complexity levels in 545 squamates sorted by diet. **c** Discrete cosine transform analysis of multicuspid tooth labial view profiles from 75 extant and fossil squamate species, with 95% confidence ellipses for insectivorous, omnivorous, and herbivorous morphologies. Theoretical tooth profiles at the extreme positive and negative values of each axis reconstructed from the first 21 harmonic coefficients. Scalebar = 50 million years (My). Dagger = extinct taxon. Silhouettes: Phylopic (<http://phylopic.org>) courtesy of T. Michael Keese (used without modification, CC0 1.0 and CC-BY 3.0 <https://creativecommons.org/licenses/by/3.0/>), David Orr (CC0 1.0), Iain Reid (used without modification, CC-BY 3.0 <https://creativecommons.org/licenses/by/3.0/>), Alex Slavenko (CC0 1.0), and Steven Traver (CC0 1.0), and F.L. after Darren Naish (used with permission) and Ted M. Townsend (silhouette drawn from photograph, CC-BY 2.5 <https://creativecommons.org/licenses/by/2.5/deed.en>); see Methods for full license information. Source data are provided as a Source Data file.

Cretaceous, respectively), they remained marginal for dozens of millions of years (Fig. 3a, c). It is only during the Cretaceous Terrestrial Revolution (KTR, ~125–80 Ma) and, specifically, the Late Cretaceous, that the relative abundance and disparity of multiple-cusped teeth and plant-based diets started increasing.

The highest cusp numbers and true herbivorous diets became increasingly prevalent only after the Cretaceous–Paleogene (K–Pg) mass extinction. Importantly, squamate dental evolution was labile and included repeated reversals towards lower tooth complexity. Both complexity and diet changed similarly through

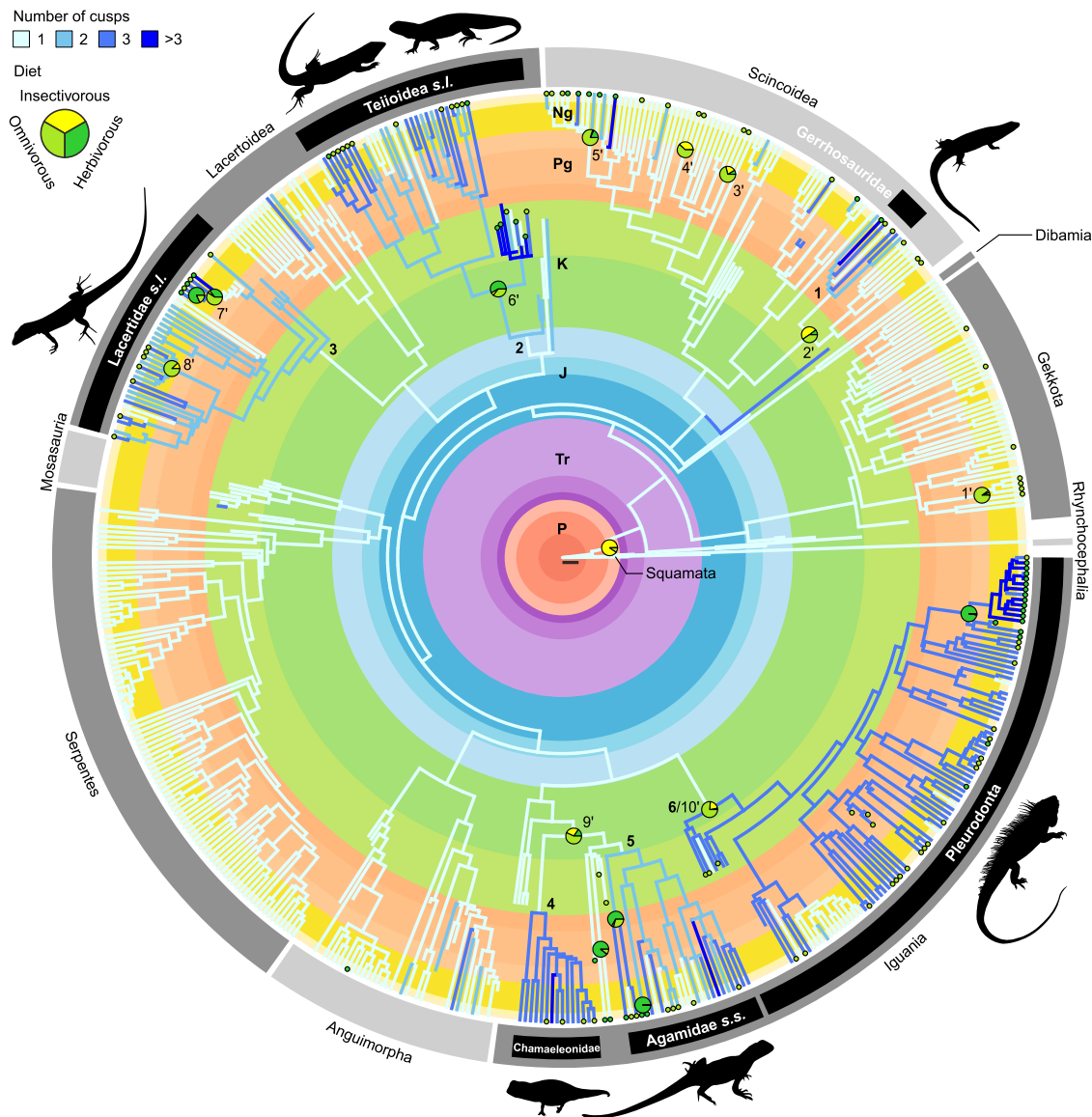


Fig. 2 Multiple independent acquisitions of multicusp teeth and plant consumption are found across squamate phylogeny. Known and maximum likelihood ancestral state reconstructions of the number of cusps (branch colours) and diet (node pie charts and branch tip small circles) in squamates. Pie charts indicate the most ancient nodes with >50% combined relative likelihood for omnivorous and herbivorous diets; also shown are the first nodes with >50% relative likelihood for herbivory within already omnivorous clades. Branch tip circles indicate omnivorous/herbivorous species. Six major clades show independent originations of multicusp teeth: 1: Gerrhosauridae (node 616; see Supplementary Fig. 1). 2: Teiioidea + Polyglyphanodontia (informally Teiioidea *sensu lato*; node 686). 3: total group Lacertidae (informally Lacertidae *sensu lato*; node 740). 4: Chamaleonidae (node 930). 5: non-Uromastycinae agamids (informally Agamidae *sensu stricto*; node 949). 6: total group Pleurodonta (node 971). Independent originations of plant consumption (isolated terminal branches not included): 1': unnamed clade including the most recent common ancestor (MRCA) to *Correlophus ciliatus* and *Rhacodactylus auriculatus* and all its descendants (node 563). 2': Cordyloidea (node 609). 3': unnamed clade including the MRCA to *Eumeces schneideri* and *Scincus scincus* and all its descendants (node 652). 4': *Chalcides* (node 657). 5': Egerniinae (node 674). 6': unnamed clade including the MRCA to *Polyglyphanodon sternbergi* and *Teius teyou* and all its descendants (node 688). 7': *Gallotia* (node 750). 8': *Podarcis* (node 765). 9': crown Acrodonta (node 929). 10': total group Pleurodonta (node 971). P: Permian. Tr: Triassic. J: Jurassic. K: Cretaceous. Pg: Paleogene. Ng: Neogene. Scalebar = 10 million years. Silhouettes: Phylopic (<http://phylopic.org>) courtesy of T. Michael Keesey (from a photograph by Frank Glaw, Jörn Köhler, Ted M. Townsend & Miguel Vences, used without modification, CC-BY 3.0 <https://creativecommons.org/licenses/by/3.0/>), Michael Scroggie (CC0 1.0), Alex Slavenko (CC0 1.0), and Jack Meyer Wood (CC0 1.0), and F.L. after Dick Culbert (silhouette drawn from photograph, CC-BY 2.0 <https://creativecommons.org/licenses/by/2.0/deed.en>), Scott Robert Ladd (silhouette drawn from photograph, CC-BY 3.0 <https://creativecommons.org/licenses/by/3.0/>), and Darren Naish (used with permission); see Methods for full license information.

much of squamate evolutionary history, though there were more changes in diet than complexity (115 vs. 92 lineages), and reversals in diet were more common than for complexity (56% vs. 44%) (Fig. 3b, d and Supplementary Fig. 6). Such flexibility is reflected in the reconstructed transition rates underlying our models of evolution for tooth complexity and diet, where higher

relative rates characterise decreases in cusp number and plant consumption compared to increases (Supplementary Fig. 7 and Supplementary Tables 3 and 4). Moreover, 38% of inferred complexity decreases were due to the simultaneous loss of two cusps or more, while multiple-cusp addition events were half (20%) as frequent. We identify two lineages (genera *Gallotia* and

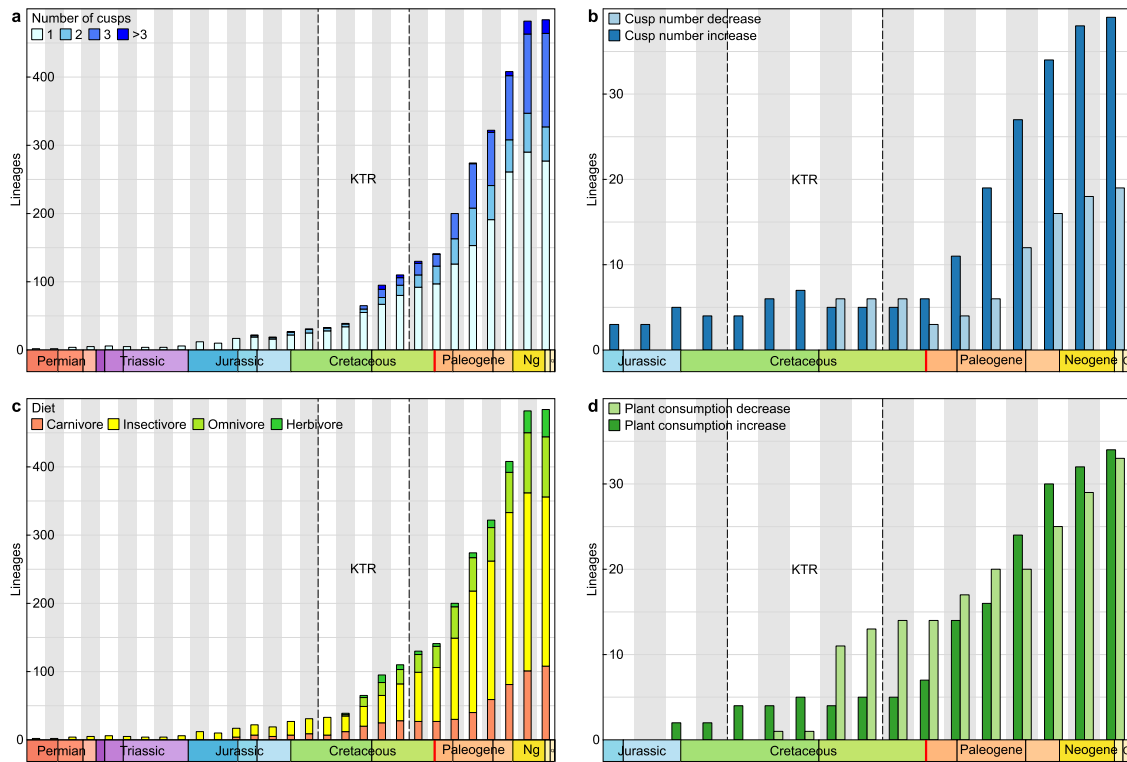


Fig. 3 Dynamics of squamate tooth complexity and plant consumption evolution. Squamate lineages sorted by cusp number (**a**, single-cusped: $n = 651$, two-cusped: $n = 145$, three-cusped: $n = 238$, more than three cusps: $n = 33$) and diet (**c**, carnivore: $n = 246$, insectivore: $n = 556$, omnivore: $n = 203$, herbivore: $n = 62$) per 10 million year-time bins based on maximum likelihood ancestral state reconstructions. Lineages showing increasing ($n = 61$) or decreasing ($n = 31$) tooth complexity (**b**) and increasing ($n = 51$) or decreasing ($n = 64$) plant consumption (**d**) per 10 million year-time bins. KTR: Cretaceous Terrestrial Revolution (-125–80 Ma). Q: Quaternary. Decreases in both cusp number and plant consumption proportion first outnumber increases during the Cretaceous Terrestrial Revolution (KTR), while the Cretaceous–Paleogene boundary (in red) shows the change towards the Cenozoic pattern of approximately twice as many cusp increases as decreases, and similar numbers of plant consumption increase and decrease from the Paleogene on. Source data are provided as a Source Data file.

Phrynosoma) in which multicuspid teeth re-evolved following earlier loss (Fig. 2 and Supplementary Fig. 6). Most often, reversals to lesser cusp numbers followed a decrease in plant consumption (52% of paired events; Supplementary Table 5), likely resulting from the relaxation of selective pressures for plant consumption.

Furthermore, we find the observed dental-dietary patterns derive from the correlated evolution of tooth complexity and plant-based diets under highly variable rates of phenotypic evolution. Our results show strong support for a correlated model of the evolution of multicuspidness and plant consumption, which assumes transition rates in one trait directly depend on character state in the other trait (log Bayes Factor = 21, Supplementary Table 6). Additionally, a model with heterogeneous character transition rates throughout the tree better fits the macroevolutionary pattern of each trait than a constant model, with the highest rates observed resulting in a relatively balanced mixture of tooth complexity and diet character states for the clades concerned (e.g., Lacertidae) (Figs. 2, 4a, b and Supplementary Table 7). We also find pronounced support for shifts in the rate of evolution of dental shape outline independent of cusp number among the 75 species with multicuspid teeth examined (log Bayes Factor = 319), with particularly high rates characterising Iguanidae (Supplementary Fig. 8). A multiple-optima Ornstein-Uhlenbeck multivariate model is largely preferred to fit tooth outline data, showing that the evolution of multicuspid tooth shapes can be explained by a dietary-

dependent adaptive process (Supplementary Tables 8–11 and Supplementary Fig. 9).

Squamate diversification dynamics. These evolutionary increases in tooth complexity and plant consumption appear to have contributed to the diversification of Squamata. Using models with variable rates of diversification implemented in a Bayesian framework through a reversible jump Markov Chain Monte Carlo algorithm and allowing for the inclusion of fossil taxa (see Methods), we identified 18 events of increased speciation with up to an eight-fold magnitude for the focal group vs. its outgroup, including 13 shifts repeated in at least half our replicates (Fig. 4c and Supplementary Table 12). Five speciation increases—all inferred in half of replicates or more—coincide exactly with increases in tooth complexity (Polyglyphanodontia and a subclade of Iguanidae), plant consumption (Egerniinae and *Podarcis*, both towards omnivory) or both (total group Pleurodonta, see Fig. 4c and Supplementary Table 12), and five are just one node away from such increases (Polyglyphanodontia, total group Teiioidea, crown Teiioidea, the previous Iguanidae subclade, and one of its own sub-clades, see Supplementary Table 13). The equivalent results for decreases are two (total group *Gallotia*, in only two replicates, and genus *Phrynosoma*, in all replicates, see Fig. 4c and Supplementary Table 12) and three lineages, respectively (Polyglyphanodontia, crown Pleurodonta, and a subclade of Liolaemidae, see Supplementary Table 13). Furthermore, five of

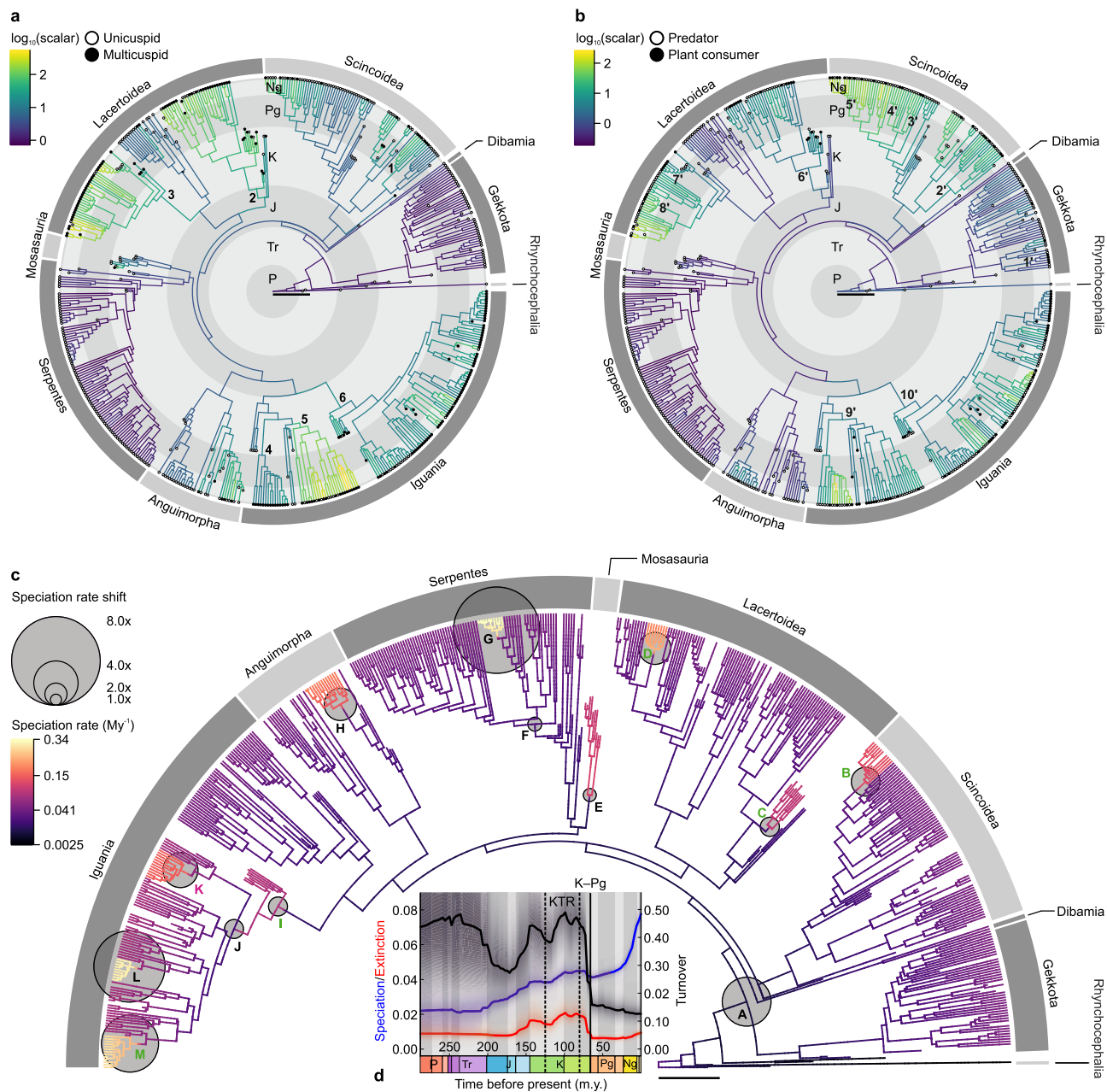


Fig. 4 Dental-dietary rates of phenotypic evolution and squamate diversification patterns. Log-transformed averaged rate scalars of the character transition rates of tooth complexity (**a**) and diet (**b**) across squamates. Positive values (i.e., rate scalar > 1) indicate increased relative transition rates. **c** Rates of squamate speciation for one maximum shift credibility configuration (MSC) out of ten similar independent replicates. Thirteen rate shifts (A–M) present in at least five MSC replicates are indicated proportionally to their magnitude compared to the background rate. **d** Mean rates of squamate speciation and extinction (in My⁻¹), and turnover (extinction/speciation) through time; see also Supplementary Fig. 10. Shaded areas: 95% confidence interval. 1: Gerrhosauridae (node 616; see Supplementary Fig. 1). 2: Teiioidea + Polyglyphanodontia (informally Teiioidea *sensu lato*, node 686). 3: total group Lacertidae (informally Lacertidae *sensu lato*, node 740). 4: Chamaeleonidae (node 930). 5: non-Uromastycinae agamids (informally Agamidae *sensu stricto*, node 949). 6: total group Pleurodonta (node 971). 1': unnamed clade including the most recent common ancestor (MRCA) to *Correlophus ciliatus* and *Rhacodactylus auriculatus* and all its descendants (node 563). 2': Cordyloidea (node 609). 3': unnamed clade including the MRCA to *Eumeces schneideri* and *Scincus scincus* and all its descendants (node 652). 4': *Chalcides* (node 657). 5': Egerniinae (node 674). 6': unnamed clade including the MRCA to *Polyglyphanodon sternbergi* and *Teius teyoi* and all its descendants (node 688). 7': *Gallotia* (node 750). 8': *Podarcis* (node 765). 9': crown Acrodonta (node 929). 10': total group Pleurodonta (node 971). A: crown Squamata. B: Egerniinae. C: Polyglyphanodontia. D: *Podarcis*. E: Mosasauria. F: crown Alethinophidia. G: *Chilabothrus*. H: *Varanus*. I: total group Pleurodonta. J: crown Pleurodonta. K: *Phrynosoma*. L: unnamed clade including the most recent common ancestor (MRCA) of *Liolaemus darwini* and *L. scapularis* and all its descendants. M: unnamed clade including the MRCA of *Ctenosaura quinquecarinata* and *Cyclura cornuta* and all its descendants. Direct correspondences between increased speciation and increased (green) or decreased (magenta) tooth complexity/plant consumption are indicated. P: Permian. Tr: Triassic. J: Jurassic. K: Cretaceous. Pg: Paleogene. Ng: Neogene. Q: Quaternary. KTR: Cretaceous Terrestrial Revolution (~125–80 Ma). K–Pg: Cretaceous–Paleogene extinction event (66 Ma). Scalebars = 50 million years.

the 13 shifts towards increased speciation occurred within a single clade—Pleurodonta—coinciding and following the evolution of three-cusped teeth and omnivory. Notable deviations include Mosasauria, crown Alethinophidia, *Chilabothrus*, and *Varanus* (see Fig. 4c and Supplementary Fig. 12), four clades of predatory squamates with single-cusped teeth that experienced marked increases in speciation rate. Over the whole of Squamata, the mean rate of speciation locally peaked in the Late Cretaceous, towards the end of the KTR. Mean extinction and turnover (extinction/speciation) reached their absolute peak during the same period (Fig. 4d and Supplementary Fig. 10), and a local maximum in species diversity resulted immediately following the end of the KTR, in the Campanian (Supplementary Fig. 11). We further tested the apparent association between diversification shifts and transitions of cusp number and diet using a hidden state trait-dependent model of speciation and extinction. Results from this model (Supplementary Table 14 and Supplementary Fig. 12) suggest each trait (tooth complexity and diet) contributed considerably to the diversification of the group as a whole and particularly of non-ophidian squamates—with rates of speciation and extinction increasing with transitions to multicuspidness or plant-based diets—despite the influence of unobserved factors beyond our study. Combining these results, we propose plant consumption and tooth complexity changes—principally increases—were critical innovations for squamate evolution.

Discussion

The evolution of tooth complexity in Squamata encompasses multiple independent radiations defined by increasingly complex teeth. This mirrors patterns of mammalian diversification, in which stem mammals show repeated independent evolutions of multicuspid teeth through the Palaeozoic and Mesozoic^{4,12,13}, the key adaptations of tribosphenic or pseudo-tribosphenic molars separately originated in the Jurassic²⁴, and quadritubercular molars with a hypocone appeared multiple times in the Cenozoic^{11,25,26}. It differs from the mammalian pattern, however, in that the most recent common ancestor (MRCA) of Mammalia was unicuspid¹². Here, we reconstruct the MRCA of Squamata as unicuspid and infer at least 24 independent acquisitions of multicuspidness in squamate lineages, a number that might increase in future studies including additional extant or fossil specimens. Squamate tooth evolution was also not mainly unidirectional as in mammals, with numerous lineages losing tooth complexity, including reversals to the ancestral unicuspid condition, though never reaching complete loss of teeth. Moreover, tooth complexity at times subsequently re-emerged within lineages that previously underwent such reversals, in opposition to Dollo's law²⁷. Despite the lack of a similar large-scale phylogenetic assessment, studies suggest relatively few mammalian lineages experienced reversals towards reduced tooth complexity (including complete tooth loss)^{28–30}, and even fewer re-evolved cusps once lost³¹. These discrepancies highlight that how often dental complexity evolves is arguably less critical than how complexity emerges in a clade. The single origin of the tribosphenic molar led to therian mammals achieving degrees and patterns of tooth complexity unparalleled across vertebrates and considerable ecological diversification during the Cenozoic. In contrast, by the Late Cretaceous several squamate lineages had evolved multicuspid teeth, even reaching uniquely complex morphologies³². Yet, squamates never recovered some of these morphologies and failed to increase dental complexity further following the K–Pg extinction, meaning that most of squamate dental diversity can largely be described by the sole variation of cusp number. Other factors beyond the scope of this study are nevertheless noteworthy. Most notably, squamate multicuspid

morphologies may differ in the accommodation of cusp placement on the crown: most often, along the mesial-distal axis with varying degrees of lateral crown compression or, less commonly, bucco-lingually through an extension of the crown such as in extant Teiidae (e.g., *Teius teyou*³³) or extinct Polyglyphanodontia (e.g., *Peneteius aquilonius*³²). Few squamates are distinguished by a degree of occlusion between tooth rows^{32,34}, which may actively contribute to tooth morphology through dental wear³⁵. Morphological heterodonty along the dental row is another important feature of species bearing multicuspid teeth, ranging from an antero-posterior gradient of multicuspidness to regionalisation resembling the morpho-functional units of mammalian dentitions (e.g., *Tupinambis teguixin*³⁶). These differences among multicuspid dentitions allow for increased dietary specialisation, typically towards higher plant consumption.

We confirm here across the whole of Squamata the link noted previously between plant-eating squamates and a specialised, typically more complex dentition¹⁷, similar to those hypothesised or discovered for early tetrapods⁴, crocodyliforms⁶, and mammals⁵. The generality of these findings suggests similar ecological and dietary selective pressures for complex dental phenotypes operate across all tetrapods. We find strong support for correlated adaptive evolution of multicuspidness and plant consumption in Squamata as a whole, and that both traits promoted increased diversification, with increased speciation coinciding with increasing tooth complexity and/or plant consumption in five major squamate groups (Egerniinae, Polyglyphanodontia, *Podarcis*, Pleurodonta, and a subclade of Iguanidae). Factors previously identified as influential for squamate diversification include global temperatures^{37,38}, latitude³⁹, and habitat^{40,41}. In broad accordance with previous reports^{42–44}, we identify locally intense diversification dynamics and a diversity peak during the late Cretaceous, a phase shift at the Cretaceous–Paleogene (K–Pg) boundary, and an increase in diversity during the Cenozoic. We also note some discrepancies in more specific patterns such as the degree of Cenozoic diversification, likely stemming from differences in methods (tree-based vs. time series) and known biases like the pull of the Present. In agreement with other recent studies⁴⁵, we propose environmental factors such as the floral turnovers towards angiosperm dominance of the Cretaceous Terrestrial Revolution^{46,47} and the subsequent evolution of angiosperm-dominated environments (notably rainforests) in the Cenozoic^{48,49} as the most plausible drivers of increasing plant consumption in squamate evolution⁵⁰. The Cretaceous saw the diversification of omnivores and herbivores among several tetrapod clades, including ornithischian and theropod dinosaurs^{7–9}, crocodyliforms⁶, testudines⁵¹, and multituberculates¹³. Specifically, during the KTR, squamate speciation locally peaked in the Campanian, and both extinction and turnover (here defined as the ratio of extinction to speciation rate) were overall highest. All three metrics drop in the Maastrichtian and across the Cretaceous–Paleogene boundary, a pattern reminiscent of the Maastrichtian decline in speciation rates recently identified in non-avian dinosaurs⁵² and suggesting the K–Pg extinction event had less of an effect on squamate diversification dynamics than the KTR. These KTR diversification shifts coincide with the majority of the only period where reductions in both tooth complexity and plant consumption outnumber increases, suggesting a rapidly shifting set of available dietary niches as previously proposed for mammals of the same time⁵³. Through the KTR, squamates experienced steadily increasing phenotypic disparity towards a peak in the latest Cretaceous⁵⁴, a period during which they were also arguably most ecologically innovative (see, e.g., mosasaurs^{55,56}, polyglyphanodonts³²). Nevertheless, important ecological diversification also occurred during the Cenozoic,

which saw the most originations of plant consumption, though without resulting in a diversity of herbivores comparable to mammals. Reductions of squamate cusp number most often followed plant consumption reductions, suggesting relaxed selective pressures on diet enabled the loss of tooth complexity, as with mammals^{29,30}. However, selective pressures on squamate teeth may not be as intense as for mammals. Most plant-eating squamates still consume insects⁵⁷, suggesting that, unlike in Mammalia, no hyper-specialist ratchet operated^{58,59}. Besides, predatory squamates with single-cusped teeth—snakes in particular—also noticeably contributed to the diversification of the group during the Cenozoic⁶⁰, though without reaching the intensity of mammalian radiations^{43,44}. This supports the contribution of factors other than tooth complexity and plant consumption to the diversification of certain squamate groups and emphasises the unique macroevolutionary dynamics of snakes, although key dental-dietary adaptations like the venom-delivering fangs of Colubroidea^{60–63}, the ziphodont teeth of monitors^{64–66}, or the piercing, cutting, and crushing teeth of mosasaurs^{56,67–69} may also have contributed to the success of these groups.

The patterns of squamate dental complexity evolution we observe offer a valuable counterpoint to the mammalian picture, exemplifying dental-dietary adaptations that responded to similar selective pressures, while resulting in more labile dental complexity throughout evolution. Despite vertebrates sharing a basic tooth gene-network¹⁵, mammal teeth are more integrated structures, less prone, through developmental fine-tuning and intense selective pressures, to loss of complexity, though also capable of accumulating significantly more variance and reaching farther phenotypic extremes over time⁷⁰. Since such finely tuned dental morphologies and precise occlusion have a critical role in ensuring mammals meet their high-energy needs², endothermy may limit the possibilities of mammalian dental simplification compared to ectothermic squamates. Several dental developmental differences to mammals can be suggested to explain why squamates did not fall into a developmental complexity trap⁷¹, but instead evolved complex teeth highly liable to developmental instability and simplification^{72,73}. These include simpler, less compartmentalised expression of dental development genes during tooth formation^{16,19}, a less complex morphological starting point than mammal teeth¹², and potentially simpler and/or looser gene regulatory networks¹⁵. We propose these characteristics of squamates explain both the evolutionary lability of their dental complexity and diet, and the near-complete absence of mammal-like teeth in over 250 million years of squamate history³².

Methods

Phylogenies. We gathered our own observations and reports from the literature on cusp number and diet for 548 species (429 extant species and 119 fossil species equally distributed between Mesozoic and Cenozoic). The data include all major squamate groups plus squamate stem taxa ($n = 545$)—including the oldest known squamate *Megachirella wachleri*, two rhynchocephalians (the extant *Sphenodon punctatus* and the fossil *Gephyrosaurus bridensis*), and a stem lepidosaurian (*Sophineta cracoviensis*). To provide a phylogenetic framework for our analyses, we assembled an informal super-tree⁷⁴ for the 548 taxa. For topology we followed the total evidence phylogeny of Simões et al.²³—the first work to find agreement between morphological and molecular evidence regarding early squamate evolution. The same source provided time calibrations for *Sophineta cracoviensis*, fossil and extant Rhynchocephalia, stem squamates and crown squamate groups. Using additional sources, we gathered complementary information on the stem and crown of Gekkota^{75–77}, Dibamia⁷⁷, Scincoidea^{76,77}, Lacertoidea^{76–82}, including Polyglyphanodontia^{76,83}, Mosasauria⁷⁶, Serpentes^{76,77}, Anguimorpha^{76,77}, and Iguania^{76,77,84–86}. We followed Simões et al.²³ for the relationships of *Najash* and *Pachyrhachis*, and Pyron⁷⁶ for the placement of *Haasiophis* and *Eupodophis* (which were not sampled by Simões et al.²³), thus reflecting both placements for simoliophiid snakes. To avoid over-sampling Liolaemidae, we randomly selected species according to relative abundance of dietary categories within the group⁵⁰ and of liolaemids among squamates. In the absence of time-calibrated phylogenetic information, we used temporal ranges from the Paleobiology Database ([https://](https://www.paleobiodb.org)

www.paleobiodb.org) and checked accuracy by comparison with cited sources. Each squamate group stated above was grafted onto the backbone of the Simões et al.²³ phylogeny according to its proposed calibrations. Node calibrations falling within the 95% highest posterior density for the corresponding node in the Simões et al.²³ phylogeny were kept unchanged. Where a calibration fell beyond that range, the calibration of Simões et al.²³ was preferred. For taxa and nodes not included in Simões et al.²³ and with phylogenetic data lacking time-calibration, we used the code of Mitchell et al.^{87,88} to generate calibrations based on last appearance dates and estimated rates of speciation, extinction, and preservation. The method—derived from Bapst⁸⁹—allows the stochastic estimation of node age based on the inferred probability of sampling a fossil and probability density of unobserved evolutionary history, though nodes are sampled downwards towards the root rather than upwards from it. We used preliminary BAMM 2.6⁸⁷ runs not including the taxa concerned to generate estimates of speciation and extinction rates and selected a preservation rate of 0.01 (see below). Our tree includes 27 unresolved nodes, denoting phylogenetic uncertainty. For methods requiring a fully dichotomous tree, we used the function `multi2di` in `ape` 5.3⁹⁰ for R 3.6.1⁹¹ to generate a random dichotomous topology. Because of the sensitivity of BAMM to zero-length branches, we then used the method of Mitchell et al.⁸⁸ to generate non-zero branch lengths in randomly resolved polytomies with fossil taxa. We used the same randomly resolved and calibrated tree in all analyses requiring a dichotomous tree. Node and branch nomenclature for the polytomous and dichotomous tree are available in Supplementary Figs. 1–4. We referred to the August 12th, 2019 version of the Reptile Database (<http://www.reptile-database.org>) and the Paleobiology Database (<https://www.paleobiodb.org>) for taxonomical reference of extant and fossil species (respectively).

Dietary data. We followed Meiri⁹² and Pineda-Munoz & Alroy⁹³ for dietary classification. Accordingly, when quantitative dietary data were available, we classified species based on the main feeding resource in adults (i.e., >50% of total diet in volume⁹³). Species consuming >50% plant material were classified as herbivores. We followed Meiri⁹² and Cooper & Vitt⁹⁴ in defining omnivorous diets as including between 10 and 50% of plants, to account for accidental plant consumption by some predators. Among predators, carnivores are defined as feeding mostly on vertebrates. Predators consuming primarily arthropods and molluscs are insectivores. We could find no published dietary hypothesis for 64 out of 119 fossil species, which we assigned to the most plausible of our diet categories based on tooth complexity and the diets of closely related taxa (see Supplementary Data 3).

Geometric morphometrics. Specimens of 75 species were selected to represent all major groups of squamates with multiple-cusped teeth and based on the quality of the material available. We extracted two-dimensional outlines for geometric morphometric analyses (Supplementary Data 4) from 52 X-ray computed microtomography scans (microCT-scans), 12 photographs, 10 anatomical drawings of specimens, and one scanning electron microscopy (SEM) image. Sources included the literature, the Digital Morphology (DigiMorph) library, four new photographs, and four new microCT-scans (see below and Supplementary Data 3).

To analyse morphological variation of tooth shapes, we collected two-dimensional open outlines of a left upper posterior maxillary multicuspid tooth in labial view with ImageJ 1.47v⁹⁵. We chose whenever possible the tooth with the most numerous cusps in the quadrant. If no left maxillary tooth was sampled or suitable for tracing an outline, we referred to the right quadrant or lower jaws and mirrored the outline adequately to retain the same orientation. We used the EqualSpace function from PollyMorphometrics 10.1⁹⁶ for Mathematica 10⁹⁷ to normalise teeth outlines as sets of 200 equally spaced points based on Bézier splines functions.

We used Momocs 1.3.0⁹⁸ for R⁹¹ to perform geometric morphometric analyses of tooth outlines. We first applied a Bookstein alignment⁹⁹ and, for each outline, computed by Discrete Cosine Transform (DCT) the first 21 harmonic amplitudes¹⁰⁰. Harmonic coefficients were then processed by Principal Component Analysis (PCA)¹⁰¹. We limited graphical representation of the PCA to its first two axes, accounting for 89% of all morphological variation. To determine the significance of our dietary grouping, we fitted a phylogenetic multivariate linear model using penalised likelihood (PL)^{102,103} on all PC scores using mvMORPH 1.1.4¹⁰⁴ for R⁹¹. As we sampled only two carnivorous species, we added these to our insectivorous sample ($n = 50$), so making a predatory group, to avoid spurious conclusions arising from groups with extremely low-sample sizes. Model fit was performed using Pagel's λ ¹⁰⁵ to jointly estimate the phylogenetic signal in model residuals. We then used a one-way phylogenetic PL-MANOVA to evaluate overall differences between dietary groups. To examine how dietary groupings best separate, we computed a discriminant analysis (DFA) on the regularised variance-covariance matrix of the fitted model. To test between-group differences, we used general linear hypothesis testing through contrast coding. We fitted a model for which each group was explicitly estimated to test compound contrasts. Lastly, we used mvMORPH to fit Brownian Motion (BM), early burst (EB), and Ornstein-Uhlenbeck (OU)¹⁰⁶ multivariate models of continuous trait evolution on the first five PC axes, representing over 95% of total variance and compared relative fit using Akaike weights¹⁰⁷ (see Supplementary Tables 10 and 11).

Ancestral character state reconstructions. We reconstructed the evolution of cusp number and diet using maximum likelihood (ML) ancestral character state reconstruction under a time-reversible continuous Markov transition model^{108,109} as implemented in *phytools* 0.6–99¹¹⁰. We retrieved marginal ancestral states at the nodes of the tree with the re-rooting algorithm from the same package¹¹¹ and generated a model of character evolution by averaging three character transition matrices (all transitions allowed with either all rates different, symmetrical rates, or equal rates) according to their respective fit through Akaike-weights model averaging¹⁰⁷ (see Supplementary Tables 3 and 4). Finally, we used stochastic character mapping (1,000 simulations) to compute the most likely character states at each node based on the model-averaged transition matrix¹¹². In contrast with tooth complexity ancestral states reconstructions, extant data allow the formulation of informed hypotheses on possible dietary transitions in squamates. Insects are an important food resource for the juveniles of many squamate species, and several extant species of plant consumers show an ontogenetic dietary shift from insectivorous juveniles to omnivorous or herbivorous adults^{57,94,113,114}. Moreover, extant data show that predatory squamates may rely on plant material depending on environmental conditions^{50,94,115–117}. Therefore, it has been hypothesised that squamate plant consumption originated in predatory animals, which evolved increasingly more plant-based diet through time under selective pressure^{50,94}. We thus chose to test a specific hypothesis of dietary transitions against naive models and base our reconstructions on the best-performing model. We compared the respective fit of three default models (all transitions allowed) to three variants of our hypothesis of dietary transitions (limiting transitions to carnivore-insectivore, insectivore-omnivore, and omnivore-herbivore, with three transition rate regimes) and selected the model with highest relative fit (i.e., the custom model with all rates different) to retrieve ancestral states at the nodes (see Supplementary Tables 3 and 4). Through the same approach, we generated ancestral character reconstructions with three states (predatory, omnivorous, and herbivorous; see Supplementary Tables 8 and 9), which we then pruned to the geometric morphometric dataset to generate a mapping of regimes for a multi-peak OU multivariate model based on diet (see above; Supplementary Fig. 9). Based on the four-state diet and tooth complexity ancestral reconstructions, we gathered a list of changes in cusp number and plant consumption. Subsequently, we identified pairs of increases or decreases in both traits belonging to the same phylogenetic path (the unique succession of branches connecting a descendant lineage to one of its ancestors) and noted whether each initiated by a change in cusp number, plant consumption, or whether both changes happened on the same branch.

Tests of correlated evolution. We used *BayesTraits* 3.0.2 (www.evolution.rdg.ac.uk) to run Markov Chain Monte Carlo (MCMC) models of evolution of tooth complexity and diet with independent or correlated (i.e., assuming rates of transition in one trait depend on the character state of the other) rates of character transition. To improve rate estimations with our discrete dataset, in each run we scaled our tree to obtain an average branch length of 0.1 (i.e., scaling factor = 5.017e-3) as recommended by the software manual. Owing to method limitations, we transformed our discrete tooth complexity and diet characters into binary traits (teeth bearing one cusp vs. two cusps or more, and carnivores and insectivores (predators) vs. omnivores and herbivores (plant consumers), respectively). We computed two independent runs, each with four independent chains run for 110,000,000 iterations with default rate priors. We discarded the first 10,000,000 iterations as burn-in. We sampled parameters every 10,000 iterations and checked each chain for convergence (through visual examination) and large effective sample size (using CODA 0.19-3¹¹⁸ for R⁹¹). We used a steppingstone sampler¹¹⁹ to retrieve the marginal likelihood of each model (250 stones, each run for 10,000 iterations), which we compared with a log Bayes Factor to provide a measure of relative support of each model¹²⁰. Analyses of the following combinations of different binarizations of the dataset yielded similar results, i.e., correlated evolution of cusp number and diet: one or two cusps vs. three cusps or more combined with carnivores and insectivores vs. omnivores and herbivores, and one to three cusps vs. more than three cusps combined with herbivores vs. other diets. As expected, a correlated model was weakly or not supported for other combinations (Supplementary Table 6).

Rates of phenotypic evolution. We estimated the evolutionary rate of tooth shape change through the variable rates model of *BayesTraits* 3.0.2^{121,122}. In this approach, a reversible-jump Markov Chain Monte Carlo (rjMCMC) algorithm is used to detect shifts in rates of continuous trait evolution—modelled by a Brownian motion (BM) process—across the branches of a phylogenetic tree. This is achieved by estimating the location of the shifts in rates (the product of a homogeneous background rate with a set of rate scalars) by using two different proposal mechanisms (one updating one branch at a time and one updating complete subclades). We used the default gamma priors on rate scalar parameters. Support for rate heterogeneity was then further confirmed by comparing the fit of the variable rates model against a null single-rate Brownian model. Here, we ran a variable rates model and a homogeneous Brownian model on the scores of the first 12 pPC axes from our phylogenetic PCA of tooth outlines, accounting for over 99% of the total variance. As PC axes can be correlated in a phylogenetic context, we

used the phylogenetic PC scores to remove evolutionary correlations^{123,124}. We ran a phylogenetic principal component analysis (pPCA)¹²⁴ on the first 21 harmonics obtained by DCT using *phytools* 0.6–99¹¹⁰ for R⁹¹. As for the original PCA, we found the two first pPC axes accounted for the largest part of all morphological variation (83% of cumulative variance). All parameters used were the same as for the correlated evolution tests (see above): two independent runs, four independent chains per run, 110,000,000 iterations, 10% burn in, default priors, rescaling factor = 3.206e-3, sampling every 10,000 iterations, convergence and sample size checks, steppingstone sampler with 250 stones run for 10,000 iterations. Finally, we plotted our species tree (using *phytools* 0.6–99¹¹⁰, *ggtree* 1.8.1¹²⁵, and *viridis* 0.5.1¹²⁶ for R⁹¹) with branches scaled by the averaged rate scalars across posterior samples (returned by the Variable Rates Post Processor; <http://www.evolution.reading.ac.uk/VarRatesWebPP/>), thus indicating the relative deviation from the background rate of change.

Likewise, we used a variable rates model approach on discrete data to detect heterogeneity in character transition rates for tooth complexity and diet. The variable rates model operates on discrete data by breaking the assumption of a single character transition rate matrix defined for the entire tree, which it achieves by rescaling this transition matrix in different parts of the tree using an rjMCMC algorithm. As for continuous data, the process generates a posterior distribution of scalars for each branch, and comparison with a null MCMC model with a constant transition matrix allows evaluation of support for heterogeneity in the strength of character transition rates. We ran the variable rates and null models similarly to tooth shape data (see above), using binarized tooth complexity and dietary data to avoid over-parameterisation. The variable rates post processor returned the averaged branch rate scalars used to plot the tree according to local deviations from the background transition matrix. The large variances returned by the post processor for some rate scalars, however, denote a relatively complex model to fit and warrant adequate caution in interpreting absolute rate scalar values, though relative rate differences should be fully representational. For clarity, we coloured each branch according to a common log-transformed scale. We again tested alternative binarizations of diet and tooth complexity and found support for a variable rates model for the alternative binarization of diet and one other binarization of tooth complexity (one or two cusps vs. three cusps or more) (Supplementary Table 7).

Models of diversification. We fitted different trait-dependent models of speciation and extinction (BiSSE, HiSSE) and associated trait-independent null models with *hisse* 1.9.5¹²⁷ for R⁹¹, for which we compared relative fit using Akaike weights¹⁰⁷. In addition, we used an rjMCMC algorithm with BAMB 2.6⁸⁷ and BAMBtools 2.1.6 for R⁹¹ to model rates of speciation and extinction independently from trait evolution on a random resolution of our super-tree (see above). This is currently the only available method allowing branch-specific estimation of diversification rates on non-ultrametric trees (i.e., including fossil taxa) by using a fossilised birth-death process⁸⁷, whereas recent and more robust approaches such as ClDS¹²⁸ cannot handle them. The choice of a tree-based method over approaches based on time series (such as PyRate¹²⁹) allows the direct comparison of diversification rates with Maximum Likelihood ancestral state reconstructions and branch-specific rates of phenotypic evolution (see above) and provides an assessment of diversification dynamics not only through time, but across clades. This removes ambiguity in defining time series for different clades while simultaneously coping with issues of poor fossil records. We produced ten independent replicates, each with four independent chains run for 20,000,000 generations. We used priors generated by the *setBAMB*priors function of BAMBtools (expectedNumberOfShifts = 1.0; lambdaInitPrior = 10.2511191939331; lambdaShiftPrior = 0.00400165322948176; muInitPrior = 10.2511191939331), a preservation rate prior of 0.01 to reflect the sampling biases affecting the squamate fossil record⁴² in the absence of any published or reported estimation, and a global sampling fraction of 0.048 accounting for our sampling relative to the total diversity of living and extinct squamates referenced in both the Reptile Database (<http://www.reptile-database.org>) and the Paleobiology Database (<https://www.paleobiodb.org>). We set a 10% burn-in and checked convergence through visual examination and effective sample size with CODA 0.19-3¹¹⁸. As we encountered many equiprobable configurations, for each run we computed the maximum shift credibility (MSC) configuration and extracted speciation and extinction rates for clades defined by each node immediately above a shift, plus mean rates outside these clades (background rate). We then calculated a mean shift magnitude for each clade using the ratio of its mean speciation rate over the mean background rate¹³⁰. To control for the influence of aquatic taxa during the KTR, we repeated analyses on a tree devoid of Cretaceous aquatic taxa (ten mosasaur and three snakes) and found no changes to our results. To allow the comparison of shifts in diversification rate (inferred along branches) and character transitions (reconstructed at nodes only), we assigned each shift to the node immediately above it (Supplementary Tables 12 and 13).

Statistics. We performed all univariate non-parametric tests using *rcompanion* 2.3.25 (<https://www.rcompanion.org>) and the base stat package in R 3.6.1⁹¹. All effect sizes¹³¹ and their 95% confidence intervals were computed by bootstrap

over 10,000 iterations. Sample size for all tests is $n = 548$. A Kruskal–Wallis H test¹³² on tooth complexity levels among squamate dietary categories showed a statistically significant effect of diet on the level of tooth complexity ($\chi^2 = 144.27$, $df = 3$, p -value = 4.5×10^{-31} , $e^2 = 0.26$ [0.20, 0.34]). Post hoc pairwise two-sided Wilcoxon–Mann–Whitney tests^{133,134} showed statistically significant differences between all dietary categories (see Supplementary Table 1 for full reporting).

We used mvMORPH 1.1.4¹⁰⁴ for R^2 to perform regularised phylogenetic one-way multivariate analyses of variance (MANOVA) and multivariate general linear hypothesis tests in a penalised likelihood framework^{102,103}. For each test, we assessed significance with a one-sided Pillai trace test over 10,000 permutations of the Pillai trace¹³⁵ obtained through regularised estimates^{102,103}. A regularised phylogenetic one-way MANOVA on the principal component scores of 75 tooth outlines showed statistically significant differences in two-dimensional (2D) tooth shape between diets ($V = 1.04$, p -value = 0.001). We then used general linear hypothesis tests to evaluate simple and compound contrasts between groups, of which all but one were statistically significantly different (see Supplementary Table 2 for full reporting).

Two-sided Wilcoxon–Mann–Whitney tests^{133,134} on speciation and extinction rates inferred using the best-performing trait-dependent model of diversification (see Supplementary Table 14 and Supplementary Fig. 12) show multiple-cusped taxa have both statistically significantly higher speciation and extinction rates than taxa with single-cusped teeth. Likewise, plant-consuming (i.e., omnivorous and herbivorous) taxa have both statistically significantly higher speciation and extinction rates than mainly predatory taxa (i.e., carnivores and insectivores) (see Supplementary Fig. 12 for full reporting).

Unless specified otherwise, all analyses and tests were replicated twice independently (ten independent replicates for the trait-independent diversification model) with consistent results.

Photographs and X-ray computed microtomography. Photographs of ten specimens were captured at the Museum für Naturkunde (Berlin, Germany). New microCT-scan data was generated for 24 specimens using a Skyscan 1272 microCT (Bruker) at the University of Helsinki (Finland), a Skyscan 1172 microCT (Bruker) at the University of Eastern Finland (Kuopio, Finland), and a Phoenix nanotom CT (GE) at the Museum für Naturkunde (Berlin, Germany). Three-dimensional surface renderings were generated using Amira 5.5.0¹³⁶.

Specimen collection. Specialised retailers provided specimens of five species (see Supplementary Data 3). The Laboratory Animal Center (LAC) of the University of Helsinki and/or the National Animal Experiment Board (ELLA) in Finland approved all reptile captive breeding (license numbers ESLH-2007-07445/ym-23 and ESAVI/7484/04.10.07/2016).

Art credits. Figure 1a (top to bottom): Steven Traver (CC0 1.0), F.L. after Ted M. Townsend (silhouette drawn from photograph, CC-BY 2.5 <https://creativecommons.org/licenses/by/2.5/deed.en>), David Orr (CC0 1.0), F.L. after Darren Naish (used with permission), Alex Slavenko (CC0 1.0), Iain Reid (used without modification, CC-BY 3.0 <https://creativecommons.org/licenses/by/3.0/>), T. Michael Keesey (CC0 1.0), Steven Traver (CC0 1.0), T. Michael Keesey (from a photograph by Frank Glaw, Jörn Köhler, Ted M. Townsend & Miguel Vences, used without modification, CC-BY 3.0 <https://creativecommons.org/licenses/by/3.0/>). Figure 2 (counterclockwise from 90°): F.L. after Darren Naish (used with permission), F.L. after Dick Culbert (silhouette drawn from photograph, CC-BY 2.0 <https://creativecommons.org/licenses/by/2.0/deed.en>), Alex Slavenko (CC0 1.0), T. Michael Keesey (from a photograph by Frank Glaw, Jörn Köhler, Ted M. Townsend & Miguel Vences, used without modification, CC-BY 3.0 <https://creativecommons.org/licenses/by/3.0/>), Michael Croggie (CC0 1.0), Jack Meyer Wood (CC0 1.0), F.L. after Scott Robert Ladd (silhouette drawn from photograph, CC-BY 3.0 <https://creativecommons.org/licenses/by/3.0/>). See <http://phylopic.org/about/> and <https://creativecommons.org/licenses/> for additional license information.

Reporting summary. Further information on research design is available in the Nature Research Reporting Summary linked to this article.

Data availability

All datasets generated and analysed during the current study (tip-state dataset, polytomous and dichotomous versions of our phylogeny, 2D outlines) are available as Supplementary Data files 1–4. We used the Reptile Database (<http://www.reptile-database.org>) to access taxonomic information on extant species and the Paleobiology Database (<https://www.paleobiodb.org>) for taxonomy and temporal ranges of fossil species. Dietary data were extracted from the database of Meiri⁹² and the published literature (see Supplementary Data 3). CT-scan data are in part publicly available on the Digimorph database (<http://digimorph.org/>) and the published literature (see Supplementary Data 3). The remnant CT-scan data are available through N.D.-P., upon reasonable request. Source data are provided with this paper.

Received: 12 June 2020; Accepted: 27 September 2021;

Published online: 14 October 2021

References

- Bels, V. L. et al. *Biomechanics Of Feeding In Vertebrates* (Springer-Verlag Berlin Heidelberg, 1994).
- Ungar, P. S. *Mammal Teeth: Origin, Evolution, and Diversity* (JHU Press, 2010).
- Machado, J. P. et al. Positive selection linked with generation of novel mammalian dentition patterns. *Genome Biol. Evol.* **8**, 2748–2759 (2016).
- Reisz, R. R. Origin of dental occlusion in tetrapods: signal for terrestrial vertebrate evolution? *J. Exp. Zool. B Mol. Dev. Evol.* **306**, 261–277 (2006).
- Evans, A. R., Wilson, G. P., Fortelius, M. & Jernvall, J. High-level similarity of dentitions in carnivorous and rodents. *Nature* **445**, 78–81 (2007).
- Melstrom, K. M. & Irmis, R. B. Repeated evolution of herbivorous crocodyliforms during the age of dinosaurs. *Curr. Biol.* **29**, 2389–2395 (2019).
- Ösi, A., Prondvai, E., Mallon, J. & Bodor, E. R. Diversity and convergences in the evolution of feeding adaptations in ankylosaurs (Dinosauria: Ornithischia). *Hist. Biol.* **29**, 539–570 (2016).
- Strickson, E., Prieto-Márquez, A., Benton, M. J. & Stubbs, T. L. Dynamics of dental evolution in ornithomimid dinosaurs. *Sci. Rep.* **6**, 28904 (2016).
- Button, D. J. & Zanno, L. E. Repeated evolution of divergent modes of herbivory in non-avian dinosaurs. *Curr. Biol.* **30**, 158–168 (2020).
- Butler, P. M. Molarization of the premolars in the Perissodactyla. *Proc. Zool. Soc. Lond.* **121**, 819–843 (1952).
- Hunter, J. P. & Jernvall, J. The hypocone as a key innovation in mammalian evolution. *Proc. Natl Acad. Sci. USA* **92**, 10718–10722 (1995).
- Luo, Z.-X. Transformation and diversification in early mammal evolution. *Nature* **450**, 1011–1019 (2007).
- Wilson, G. P. et al. Adaptive radiation of multituberculate mammals before the extinction of dinosaurs. *Nature* **483**, 457–460 (2012).
- Carroll, S. B. Chance and necessity: the evolution of morphological complexity and diversity. *Nature* **409**, 1102–1109 (2001).
- Fraser, G. J. et al. An ancient gene network is co-opted for teeth on old and new jaws. *PLoS Biol.* **7**, e1000031 (2009).
- Richman, J. M. & Handrigan, G. R. Reptilian tooth development. *Genesis* **49**, 247–260 (2011).
- Melstrom, K. M. The relationship between diet and tooth complexity in living dentigerous saurians. *J. Morphol.* **278**, 500–522 (2017).
- Zahradnick, O., Buchtova, M., Dosedelova, H. & Tucker, A. S. The development of complex tooth shape in reptiles. *Front. Physiol.* **5**, 74 (2014).
- Landova Sulcova, M. et al. Developmental mechanisms driving complex tooth shape in reptiles. *Dev. Dyn.* **249**, 441–464 (2020).
- Jernvall, J. Linking development with generation of novelty in mammalian teeth. *Proc. Natl Acad. Sci. USA* **97**, 2641–2645 (2000).
- Jernvall, J., Kettunen, P., Karavanova, I., Martin, L. B. & Thesleff, I. Evidence for the role of the enamel knot as a control center in mammalian tooth cusp formation: non-dividing cells express growth-stimulating Fgf-4 gene. *Int. J. Dev. Biol.* **38**, 463–469 (1994).
- Harjunmaa, E. et al. On the difficulty of increasing dental complexity. *Nature* **483**, 324–327 (2012).
- Simões, T. R. et al. The origin of squamates revealed by a Middle Triassic lizard from the Italian Alps. *Nature* **557**, 706–709 (2018).
- Luo, Z.-X., Cifelli, R. L. & Kielan-Jaworowska, Z. Dual origin of tribosphenic mammals. *Nature* **409**, 53–57 (2001).
- Butler, P. M. The ontogeny of molar pattern. *Biol. Rev.* **31**, 30–69 (1956).
- Van Valen, L. M. Homology and causes. *J. Morphol.* **173**, 305–312 (1982).
- Gould, S. J. Dollo on Dollo's law: irreversibility and the status of evolutionary laws. *J. Hist. Biol.* **3**, 189–212 (1970).
- Jernvall, J. & Jung, H. S. Genotype, phenotype, and developmental biology of molar tooth characters. *Am. J. Phys. Anthropol.* **31**, 171–190 (2000).
- Davit-Béal, T., Tucker, A. S. & Sire, J. Y. Loss of teeth and enamel in tetrapods: fossil record, genetic data and morphological adaptations. *J. Anat.* **214**, 477–501 (2009).
- Charles, C., Solé, F., Rodrigues, H. G. & Viriot, L. Under pressure? Dental adaptations to termitophagy and vermivory among mammals. *Evolution* **67**, 1792–1804 (2013).
- Kurtén, B. Return of a lost structure in the evolution of the felid dentition. *Soc. Sci. Fenn. Comm. Biol.* **26**, 1–12 (1963).
- Nydram, R. L., Gauthier, J. A. & Chiment, J. J. The mammal-like teeth of the Late Cretaceous lizard *Peneteius aquilonius* Estes 1969 (Squamata, Teiidae). *J. Verteb. Paleontol.* **20**, 628–631 (2000).
- Brizuela, S. & Albino, A. M. The dentition of the neotropical lizard genus *Teius* Merrem 1820 (Squamata Teiidae). *Trop. Zool.* **22**, 183–193 (2009).

34. Throckmorton, G. S. Oral food processing in two herbivorous lizards, *Iguana iguana* (Iguanidae) and *Uromastix aegyptius* (Agamidae). *J. Morphol.* **148**, 363–390 (1976).
35. Haridy, Y. Histological analysis of post-eruption tooth wear adaptations, and ontogenetic changes in tooth implantation in the acrodontan squamate *Pogona vitticeps*. *PeerJ.* **6**, e5923 (2018).
36. Presch, W. A survey of the dentition of the macroteiid lizards (Teiidae: Lacertilia). *Herpetologica* **30**, 344–349 (1974).
37. Condamine, F. L., Rolland, J. & Morlon, H. Assessing the causes of diversification slowdowns: temperature-dependent and diversity-dependent models receive equivalent support. *Ecol. Lett.* **22**, 1900–1912 (2019).
38. Garcia-Porta, J. et al. Environmental temperatures shape thermal physiology as well as diversification and genome-wide substitution rates in lizards. *Nat. Commun.* **10**, 4077 (2019).
39. Pyron, R. A. Temperate extinction in squamate reptiles and the roots of latitudinal diversity gradients. *Glob. Ecol. Biogeogr.* **23**, 1126–1134 (2014).
40. Ricklefs, R. E., Losos, J. B. & Townsend, T. M. Evolutionary diversification of clades of squamate reptiles. *J. Evol. Biol.* **20**, 1751–1762 (2007).
41. Bars-Closel, M., Kohlsdorf, T., Moen, D. S. & Wiens, J. J. Diversification rates are more strongly related to microhabitat than climate in squamate reptiles (lizards and snakes). *Evolution* **71**, 2243–2261 (2017).
42. Cleary, T. J., Benson, R. B., Evans, S. E. & Barrett, P. M. Lepidosaurian diversity in the Mesozoic–Palaeogene: the potential roles of sampling biases and environmental drivers. *R. Soc. Open Sci.* **5**, 171830 (2018).
43. Close, R. A. et al. Diversity dynamics of Phanerozoic terrestrial tetrapods at the local-community scale. *Nat. Ecol. Evol.* **3**, 590–597 (2019).
44. Close, R. A. et al. The apparent exponential radiation of Phanerozoic land vertebrates is an artefact of spatial sampling biases. *Proc. R. Soc. B* **287**, 20200372 (2020).
45. Herrera-Flores, J. A., Stubbs, T. L. & Benton, M. J. Ecomorphological diversification of squamates in the Cretaceous. *R. Soc. Open Sci.* **8**, 201961 (2021).
46. Lloyd, G. T. et al. Dinosaurs and the Cretaceous terrestrial revolution. *Proc. R. Soc. B* **275**, 2483–2490 (2008).
47. Barba-Montoya, J., dos Reis, M., Schneider, H., Donoghue, P. C. & Yang, Z. Constraining uncertainty in the timescale of angiosperm evolution and the veracity of a Cretaceous Terrestrial Revolution. *N. Phytol.* **218**, 819–834 (2018).
48. Collinson, M. E. In *Biotic Responses To Global Change: The Last 145 Million Years* (eds Culver, S. J. & Rawson, P. F.) 223–243 (Cambridge University Press, 2000).
49. Wing, S. L. et al. Late Paleocene fossils from the Cerrejón Formation, Colombia, are the earliest record of neotropical rainforest. *Proc. Natl Acad. Sci. USA* **106**, 18627–18632 (2009).
50. Espinoza, R. E., Wiens, J. J. & Tracy, C. R. Recurrent evolution of herbivory in small, cold-climate lizards: breaking the ecophysiological rules of reptilian herbivory. *Proc. Natl Acad. Sci. USA* **101**, 16819–16824 (2004).
51. Mallon, J. C. & Brinkman, D. B. *Basilemys morrinensis*, a new species of nanhsiungchelyid turtle from the Horseshoe Canyon formation (Upper Cretaceous) of Alberta, Canada. *J. Vertebr. Paleontol.* **38**, e1431922 (2018).
52. Condamine, F. L., Guinot, G., Benton, M. J. & Currie, P. J. Dinosaur biodiversity declined well before the asteroid impact, influenced by ecological and environmental pressures. *Nat. Commun.* **12**, 3833 (2021).
53. Grossnickle, D. M. & Polly, P. D. Mammal disparity decreases during the Cretaceous angiosperm radiation. *Proc. R. Soc. B* **280**, 20132110 (2013).
54. Simões, T. R., Vernygora, O., Caldwell, M. W. & Pierce, S. E. Megaevolutionary dynamics and the timing of evolutionary innovation in reptiles. *Nat. Commun.* **11**, 3322 (2020).
55. Schulp, A. S. Feeding the mechanical mosasaur: what did *Carinodens* eat? *Neth. J. Geosci.* **84**, 345–357 (2005).
56. Longrich, N. R., Bardet, N., Schulp, A. S. & Jalil, N.-E. *Xenodens calminechari* gen. et sp. nov., a bizarre mosasaurid (Mosasauridae, Squamata) with shark-like cutting teeth from the upper Maastrichtian of Morocco, North Africa. *Cretac. Res.* **123**, 104764 (2021).
57. Winkler, D. E., Schulz-Kornas, E., Kaiser, T. M. & Tütken, T. Dental microwear texture reflects dietary tendencies in extant Lepidosauria despite their limited use of oral food processing. *Proc. R. Soc. B* **286**, 20190544 (2019).
58. Holliday, J. A. & Steppan, S. J. Evolution of hypercarnivory: the effect of specialization on morphological and taxonomic diversity. *Paleobiology* **30**, 108–128 (2004).
59. Van Valkenburgh, B., Wang, X. & Damuth, J. Cope's rule, hypercarnivory, and extinction in North American canids. *Science* **306**, 101–104 (2004).
60. Alamillo, H. *Testing Macroevolutionary Hypotheses: Diversification and Phylogenetic Implications*. (Washington State University, 2010).
61. Savitzky, A. H. The role of venom delivery strategies in snake evolution. *Evolution* **34**, 1194–1204 (1980).
62. Westeen, E. P., Durso, A. M., Grundler, M. C., Rabosky, D. L. & Rabosky, A. R. D. What makes a fang? Phylogenetic and ecological controls on tooth evolution in rear-fanged snakes. *BMC Evol. Biol.* **20**, 80 <https://doi.org/10.1186/s12862-020-01645-0> (2020).
63. Palci, A. et al. Plicidentine and the repeated origin of snake venom fangs. *Proc. R. Soc. B* **288**, 20211391 (2021).
64. Losos, J. B. & Greene, H. W. Ecological and evolutionary implications of diet in monitor lizards. *Biol. J. Linn. Soc.* **35**, 379–407 (1988).
65. D'Amore, D. C. & Blumenschine, R. J. Komodo monitor (*Varanus komodoensis*) feeding behavior and dental function reflected through tooth marks on bone surfaces, and the application to ziphodont paleobiology. *Paleobiology* **35**, 525–552 (2009).
66. Fry, B. G. et al. A central role for venom in predation by *Varanus komodoensis* (Komodo Dragon) and the extinct giant *Varanus(Megalania) priscus*. *Proc. Natl Acad. Sci. USA* **106**, 8969–8974 (2009).
67. Massare, J. D. Tooth morphology and prey preference of Mesozoic marine reptiles. *J. Vertebr. Paleontol.* **7**, 121–137 (1987).
68. Bardet, N., Suberbiola, X., Iarochène, M., Amalik, M. & Bouya, B. Durophagous Mosasauridae (Squamata) from the Upper Cretaceous phosphates of Morocco, with description of a new species of *Globidens*. *Neth. J. Geosci.* **84**, 167–175 (2005).
69. Hornung, J. J. & Reich, M. Tylosaurine mosasaurs (Squamata) from the Late Cretaceous of northern Germany. *Neth. J. Geosci.* **94**, 55–71 (2015).
70. Felice, R. N., Randau, M. & Goswami, A. A fly in a tube: Macroevolutionary expectations for integrated phenotypes. *Evolution* **72**, 2580–2594 (2018).
71. Salazar-Ciudad, I. & Jernvall, J. Graduality and innovation in the evolution of complex phenotypes: insights from development. *J. Exp. Zool. B Mol. Dev. Evol.* **304**, 619–631 (2005).
72. Hagolani, P. F., Zimm, R., Marin-Riera, M. & Salazar-Ciudad, I. Cell signaling stabilizes morphogenesis against noise. *Development* **146**, dev179309 (2019).
73. Hagolani, P. F., Zimm, R., Vroomans, R. & Salazar-Ciudad, I. On the evolution and development of morphological complexity: A view from gene regulatory networks. *PLoS Comput. Biol.* **17**, e1008570 (2021).
74. Benson, R. B. & Choiniere, J. N. Rates of dinosaur limb evolution provide evidence for exceptional radiation in Mesozoic birds. *Proc. R. Soc. B* **280**, 20131780 (2013).
75. Daza, J. D., Bauer, A. M. & Snively, E. D. On the fossil record of the Gekkota. *Anat. Rec. (Hoboken)* **297**, 433–462 (2014).
76. Pyron, R. A. Novel approaches for phylogenetic inference from morphological data and total-evidence dating in squamate reptiles (lizards, snakes, and amphisbaenians). *Syst. Biol.* **66**, 38–56 (2016).
77. Tonini, J. F. R., Beard, K. H., Ferreira, R. B., Jetz, W. & Pyron, R. A. Fully-sampled phylogenies of squamates reveal evolutionary patterns in threat status. *Biol. Conserv.* **204**, 23–31 (2016).
78. Kearney, M., Maisano, J. A. & Rowe, T. Cranial anatomy of the extinct amphisbaenian *Rhineura hatcherii* (Squamata, Amphisbaenia) based on high-resolution X-ray computed tomography. *J. Morphol.* **264**, 1–33 (2005).
79. Bolet, A. & Evans, S. E. A new lizard from the Early Cretaceous of Catalonia (Spain), and the Mesozoic lizards of the Iberian Peninsula. *Cretac. Res.* **31**, 447–457 (2010).
80. Brizuela, S. & Albino, A. M. Redescription of the extinct species *Callopiastes bicuspidatus* Chani, 1976 (Squamata, Teiidae). *J. Herpetol.* **51**, 343–354 (2017).
81. Čerňanský, A. et al. A new exceptionally preserved specimen of *Dracaenosaurus* (Squamata, Lacertidae) from the Oligocene of France as revealed by micro-computed tomography. *J. Vertebr. Paleontol.* **37**, e1384738 (2017).
82. Čerňanský, A. & Smith, K. T. Eolacertidae: a new extinct clade of lizards from the Palaeogene; with comments on the origin of the dominant European reptile group–Lacertidae. *Hist. Biol.* **30**, 994–1014 (2018).
83. Simões, T. R. et al. Reacquisition of the lower temporal bar in sexually dimorphic fossil lizards provides a rare case of convergent evolution. *Sci. Rep.* **6**, 24087 (2016).
84. Apesteguía, S., Daza, J. D., Simões, T. R. & Rage, J. C. The first iguanian lizard from the Mesozoic of Africa. *R. Soc. Open Sci.* **3**, 160462 (2016).
85. DeMar, D. G., Conrad, J. L., Head, J. J., Varricchio, D. J. & Wilson, G. P. A new Late Cretaceous iguanomorph from North America and the origin of New World Pleurodonta (Squamata, Iguania). *Proc. R. Soc. B* **284**, 20161902 (2017).
86. Pincheira-Donoso, D. et al. Hypoxia and hypothermia as rival agents of selection driving the evolution of viviparity in lizards. *Glob. Ecol.* **26**, 1238–1246 (2017).
87. Mitchell, J. S., Etienne, R. S. & Rabosky, D. L. Inferring diversification rate variation from phylogenies with fossils. *Syst. Biol.* **68**, 1–18 (2018).
88. Mitchell, J. S., Etienne, R. S. & Rabosky, D. L. Data from: inferring diversification rate variation from phylogenies with fossils (Dryad) data set. <https://doi.org/10.5061/dryad.50m70> (2018).
89. Bapst, D. W. A stochastic rate-calibrated method for time-scaling phylogenies of fossil taxa. *Methods Ecol.* **4**, 724–733 (2013).
90. Paradis, E., Claude, J. & Strimmer, K. APE: analyses of phylogenetics and evolution in R language. *Bioinformatics* **20**, 289–290 (2004).

91. R Core Team. *R: A Language and Environment for Statistical Computing*. <http://www.R-project.org/> (R Foundation for Statistical Computing, Vienna, Austria, 2019).
92. Meiri, S. Traits of lizards of the world: Variation around a successful evolutionary design. *Glob. Ecol.* **27**, 1168–1172 (2018).
93. Pineda-Munoz, S. & Alroy, J. Dietary characterization of terrestrial mammals. *Proc. R. Soc. B* **281**, 20141173 (2014).
94. Cooper, W. E. Jr & Vitt, L. J. Distribution, extent, and evolution of plant consumption by lizards. *J. Zool.* **257**, 487–517 (2002).
95. Schneider, C. A., Rasband, W. S. & Eliceiri, K. W. NIH Image to ImageJ: 25 years of image analysis. *Nat. Methods* **9**, 671–675 (2012).
96. Polly, P. D. *Geometric Morphometrics for Mathematica*. Version 10.1 (Department of Geological Sciences, Indiana University: Bloomington, Indiana, 2014). <https://pollylab.indiana.edu/software/>.
97. Wolfram, S. *Mathematica: A System For Doing Mathematics By Computer* (Addison-Wesley, Boston MA, 1991).
98. Bonhomme, V., Picq, S., Gaucherel, C. & Claude, J. Momocs: outline analysis using R. *J. Stat. Softw.* **56**, 1–24 (2014).
99. Bookstein, F. L. *Morphometric Tools For Landmark Data: Geometry And Biology* (Cambridge University Press, Cambridge, 1997).
100. Dommergues, C. H., Dommergues, J. L. & Verrecchia, E. P. The discrete cosine transform, a Fourier-related method for morphometric analysis of open contours. *Math. Geol.* **39**, 749–763 (2007).
101. Pearson, K. Principal components analysis. *Philos. Mag.* **6**, 559–572 (1901).
102. Clavel, J., Aristide, L. & Morlon, H. A penalized likelihood framework for high-dimensional phylogenetic comparative methods and an application to new-world monkeys brain evolution. *Syst. Biol.* **68**, 93–116 (2019).
103. Clavel, J. & Morlon, H. Reliable phylogenetic regressions for multivariate comparative data: illustration with the MANOVA and application to the effect of diet on mandible morphology in phyllostomid bats. *Syst. Biol.* **69**, 927–943 (2020).
104. Clavel, J., Escarguel, G. & Merceron, G. mvMORPH: an R package for fitting multivariate evolutionary models to morphometric data. *Methods Ecol.* **6**, 1311–1319 (2015).
105. Pagel, M. Inferring the historical patterns of biological evolution. *Nature* **401**, 877–884 (1999).
106. Hansen, T. F., Pienaar, J. & Orzack, S. H. A comparative method for studying adaptation to a randomly evolving environment. *Evolution* **62**, 1965–1977 (2008).
107. Burnham, K. & Anderson, D. *Model Selection And Multimodel Inference. A Practical Information Theoretic Approach* (Springer-Verlag New York, New York NY, 2002).
108. Pagel, M. Detecting correlated evolution on phylogenies: a general method for the comparative analysis of discrete characters. *Proc. R. Soc. B* **255**, 37–45 (1994).
109. Yang, Z. *Computational Molecular Evolution* (Oxford University Press, Oxford, 2006).
110. Revell, L. J. phytools: an R package for phylogenetic comparative biology (and other things). *Methods Ecol.* **3**, 217–223 (2012).
111. Yang, Z., Kumar, S. & Nei, M. A new method of inference of ancestral nucleotide and amino acid sequences. *Genetics* **141**, 1641–1650 (1995).
112. Bollback, J. P. SIMMAP: stochastic character mapping of discrete traits on phylogenies. *BMC Bioinform.* **7**, 88 (2006).
113. Pough, F. H. Lizard energetics and diet. *Ecology* **54**, 837–844 (1973).
114. Pietczak, C. & Vieira, L. R. In *Herbivores* (IntechOpen, 2017).
115. Hurtubia, J. & Di Castri, F. In *Mediterranean Type Ecosystems* 349–360 (Springer, 1973).
116. Pietruszka, R., Hanrahan, S., Mitchell, D. & Seely, M. Lizard herbivory in a sand dune environment: the diet of *Angolosaurus skoogi*. *Oecologia* **70**, 587–591 (1986).
117. Van Damme, R. Evolution of herbivory in lacertid lizards: effects of insularity and body size. *J. Herpetol.* **33**, 663–674 (1999).
118. Plummer, M., Best, N., Cowles, K. & Vines, K. CODA: convergence diagnosis and output analysis for MCMC. *R. N.* **6**, 7–11 (2006).
119. Xie, W., Lewis, P. O., Fan, Y., Kuo, L. & Chen, M.-H. Improving marginal likelihood estimation for Bayesian phylogenetic model selection. *Syst. Biol.* **60**, 150–160 (2010).
120. Gilks, W. R., Richardson, S. & Spiegelhalter, D. J. In *Markov Chain Monte Carlo In Practice* (eds Gilks, W. R., Richardson, S. & Spiegelhalter, D. J.) 1–19 (Chapman & Hall, 1996).
121. Venditti, C., Meade, A. & Pagel, M. Multiple routes to mammalian diversity. *Nature* **479**, 393–396 (2011).
122. Baker, J., Meade, A., Pagel, M. & Venditti, C. Positive phenotypic selection inferred from phylogenies. *Biol. J. Linn. Soc.* **118**, 95–115 (2016).
123. Cooney, C. R. et al. Mega-evolutionary dynamics of the adaptive radiation of birds. *Nature* **542**, 344–347 (2017).
124. Revell, L. J. Size-correction and principal components for interspecific comparative studies. *Evolution* **63**, 3258–3268 (2009).
125. Yu, G., Smith, D. K., Zhu, H., Guan, Y. & Lam, T. T. Y. ggtree: an R package for visualization and annotation of phylogenetic trees with their covariates and other associated data. *Methods Ecol.* **8**, 28–36 (2017).
126. Garnier, S. et al. *viridis - Colorblind-friendly color maps for R*. <https://doi.org/10.5281/zenodo.4679424> (R package version 0.5.1, 2018).
127. Beaulieu, J. M. & O'Meara, B. C. Detecting hidden diversification shifts in models of trait-dependent speciation and extinction. *Syst. Biol.* **65**, 583–601 (2016).
128. Maliet, O., Hartig, F. & Morlon, H. A model with many small shifts for estimating species-specific diversification rates. *Nat. Ecol. Evol.* **3**, 1086–1092 (2019).
129. Silvestro, D., Salamin, N., Antonelli, A. & Meyer, X. Improved estimation of macroevolutionary rates from fossil data using a Bayesian framework. *Paleobiology* **45**, 546–570 (2019).
130. Upham, N. S., Esselstyn, J. A. & Jetz, W. Molecules and fossils tell distinct yet complementary stories of mammal diversification. *Curr. Biol.* <https://doi.org/10.1016/j.cub.2021.07.012> (2021).
131. Kelley, T. L. An unbiased correlation ratio measure. *Proc. Natl Acad. Sci. USA* **21**, 554–559 (1935).
132. Kruskal, W. H. & Wallis, W. A. Use of ranks in one-criterion variance analysis. *J. Am. Stat. Assoc.* **47**, 583–621 (1952).
133. Wilcoxon, F. Individual comparisons by ranking methods. *Biometrics* **1**, 80–83 (1945).
134. Mann, H. B. & Whitney, D. R. On a test of whether one of two random variables is stochastically larger than the other. *Ann. Math. Stat.* **18**, 50–60 (1947).
135. Pillai, K. Some new test criteria in multivariate analysis. *Ann. Math. Stat.* **26**, 117–121 (1955).
136. Stalling, D., Westerhoff, M. & Hege, H.-C. In *The Visualization Handbook* (eds Hansen, C. D. & Johnson, C. R.) 749–767 (Butterworth-Heinemann, 2005).

Acknowledgements

We thank Ilpo Hanski and Martti Hildén (Luonnontieteellinen keskusmuseo, Helsinki, Finland) for specimen loans, Johannes Müller (Museum für Naturkunde, Berlin, Germany) for specimen loans and access to collections and CT-scanning facilities, Jessie Maisano (University of Texas, Austin, TX) for sharing data from the DigiMorph database, Arto Koistinen (University of Kuopio, Finland) and Heikki Suhonen (University of Helsinki, Finland) for access to CT-scanning facilities, Arto Koistinen, Simone Macri, Kristin Mahlow, and Filipe Oliveira da Silva for acquiring morphological data, as well as Jukka Jernvall, Mikael Fortelius, and the Helsinki Evo-Devo community for discussions. We thank Vincent Bonhomme, David Caetano, Andrew Meade, and Johnathan Mitchell for their help in implementing Momocs, HiSSE models, BayesTraits, and BAMB 2.6, respectively. We also thank Robert Espinoza for precisions on liolaemid diets. This work was supported by funds from the Integrative Life Science doctoral programme (ILS; to F.L.), the Center for International Mobility scholarship programme (CIMO; to F.L.), the University of Helsinki (to N.D.-P.), the Institute of Biotechnology (to N.D.-P.), Biocentrum Helsinki (to N.D.-P.), and the Academy of Finland (to N.D.-P.).

Author contributions

F.L., I.J.C. and N.D.-P. designed the experimental approach. F.L. and N.D.-P. collected the specimens for microCT-scanning. F.L. character-coded species from the literature and specimen data. F.L. collected tooth outline semi-landmark data. F.L. performed the research. F.L. analysed the data, with contribution from J.C., I.J.C. and N.D.-P. F.L. made the figures. F.L. produced the first draft, and F.L., J.C. and I.J.C. wrote the paper, to which all authors contributed in the form of discussion and critical comments. All authors approved the final version of the manuscript.

Competing interests

The authors declare no competing interests.

Additional information

Supplementary information The online version contains supplementary material available at <https://doi.org/10.1038/s41467-021-26285-w>.

Correspondence and requests for materials should be addressed to Fabien Lafuma, Ian J. Corfe or Nicolas Di-Poi.

Peer review information *Nature Communications* thanks Nicholas Longrich, Julio Rivera and Tiago Simões for their contribution to the peer review of this work. Peer reviewer reports are available.

Reprints and permission information is available at <http://www.nature.com/reprints>

Publisher's note Springer Nature remains neutral with regard to jurisdictional claims in published maps and institutional affiliations.



Open Access This article is licensed under a Creative Commons Attribution 4.0 International License, which permits use, sharing, adaptation, distribution and reproduction in any medium or format, as long as you give appropriate credit to the original author(s) and the source, provide a link to the Creative Commons license, and indicate if changes were made. The images or other third party material in this article are included in the article's Creative Commons license, unless indicated otherwise in a credit line to the material. If material is not included in the article's Creative Commons license and your intended use is not permitted by statutory regulation or exceeds the permitted use, you will need to obtain permission directly from the copyright holder. To view a copy of this license, visit <http://creativecommons.org/licenses/by/4.0/>.

© The Author(s) 2021